

Plasmonic Time Crystals

Joshua Feinberg*

*Department of Physics and Haifa Center for Physics and Astrophysics,
University of Haifa, Haifa 3498838, Israel*

David E. Fernandes

*University of Lisbon and Instituto de Telecomunicações,
Avenida Rovisco Pais 1, Lisboa, 1049-001, Portugal*

Boris Shapiro

*Department of Physics
Technion, Israel Institute of Technology, Haifa 32000, Israel*

Mário G. Silveirinha

*University of Lisbon and Instituto de Telecomunicações,
Avenida Rovisco Pais 1, Lisboa, 1049-001, Portugal
(Dated: July 30, 2024)*

We study plasmonic time crystals, which constitute an extension of the dielectric-based photonic time crystals to plasmonic media. A salient feature of plasmonic time crystals is their ability to support amplification of both longitudinal and transverse modes. In particular, we show that such systems support collective resonances of longitudinal modes, independently of the wave vector k . These resonances originate from the interaction between the positive and negative frequency branches of the plasmonic dispersion relation of the unmodulated system, and from the divergence of the density of states near the plasma frequency ω_p . The strongest resonance occurs at a modulation frequency of $\Omega = 2\omega_p$, associated with a direct inter-band transition. Higher-order resonances are associated with related mechanisms but at lower modulation frequencies. We demonstrate these resonances for various periodic modulation profiles, and also provide a generic perturbative formula for resonance widths in the limit of weak modulation amplitude, in the absence of losses. Our findings offer insights into using time-modulated plasmonic media to enhance optical gain.

Introduction. Temporal modulation of a material amounts to changing in time some parameters of the material. In this way, a new artificial (or *meta*-)material is created, with new and useful properties^{1,2}. In particular, if the dielectric permittivity ε of a material undergoes periodic modulation, then a photonic time crystal (PTC) is produced³. A PTC can amplify electromagnetic waves with wavenumbers k lying in its k -band gaps⁴. k -bands are analogous of the frequency bands in a spatial photonic crystal.

Generally, the concept of temporal modulation applies to arbitrary time dependence $\varepsilon(t)$. For instance, the behavior of an EM wave under sudden change of ε at some instant $t = t_0$, has been considered already in 1958⁵. The case of $\varepsilon(t)$ being a random function of time has been studied recently in^{3,6}. By now, temporal modulation of materials has become a broad and active field of research with many theoretical³⁻²⁷ and some experimental²⁸⁻³¹ works.

A few previous works have investigated some particular forms of dispersive time-crystals, focusing mainly on transverse waves^{18,32-36}. In this Letter, we extend the study of PTC to longitudinal excitations of an electron

gas. To this end, we consider a time-modulated material characterized by a time-varying host dielectric with permittivity $\varepsilon(t)$ and a time-varying electron concentration $N_0(t)$. By subjecting either one of these quantities, or both, to periodic modulations at a common frequency $\Omega = 2\pi/T$, a new type of time crystal emerges that supports plasma excitations - a *plasmonic time crystal* (PLTC).

Here, we show that plasmonic time crystals are exceptional platforms for generating optical gain. This capability stems from a collective resonance, marked by a diverging density of states, that couples plasmons with positive and negative frequencies. Such a collective resonance should occur for any type of excitation with k -independent dispersion relation, and in particular, for *longitudinal* plasmons, whose temporal modulation, to our best knowledge, has not been studied before.

The authors of the very recent work³⁷ studied temporal modulation of longitudinal optical phonons, which are the characteristic excitations in a Lorentz-type medium (a set of localized charged oscillators). The focus in³⁷ was on excitation of these longitudinal optical phonons by a charge embedded in the modulated medium.

*<https://orcid.org/0000-0002-2869-0010>

modulated plasma is governed by the Maxwell equations

$$\begin{aligned} \frac{1}{c} \frac{\partial \mathbf{B}(\mathbf{r}, t)}{\partial t} &= -\nabla \times \mathbf{E}(\mathbf{r}, t) \\ \frac{1}{c} \frac{\partial (\varepsilon(t) \mathbf{E}(\mathbf{r}, t))}{\partial t} &= \nabla \times \mathbf{B}(\mathbf{r}, t) - \frac{4\pi}{c} \mathbf{J}(\mathbf{r}, t) \end{aligned} \quad (1)$$

coupled to the linearized continuity and transport equations:

$$\frac{\partial n(\mathbf{r}, t)}{\partial t} + N_0(t) \nabla \cdot \mathbf{v}(\mathbf{r}, t) = 0, \quad (2)$$

$$\frac{\partial \mathbf{v}(\mathbf{r}, t)}{\partial t} = \frac{e}{m} \mathbf{E}(\mathbf{r}, t) - \nu \mathbf{v}(\mathbf{r}, t). \quad (3)$$

Here $n(\mathbf{r}, t) \ll N_0(t)$ is the local fluctuating part of the electron density (which rides atop the spatially uniform background electron density $N_0(t)$), $\mathbf{v}(\mathbf{r}, t)$ is the electron velocity field, and ν is a collision frequency that accounts for losses in the system. The (linearized) fluctuating part of the current is $\mathbf{J} = eN_0(t) \mathbf{v}$. The specific details of currents and fields arising from the external periodic driving fall outside our scope of interest. A possible realization of plasma with time-varying N_0 can be achieved by having an electronic ‘‘pump’’ which creates a time-varying oscillating current along, say, the z -direction ($\mathbf{J}_0 \sim \hat{\mathbf{z}}$), which induces time variation of N_0 . (See Fig.S1 of the Supplementary Material for a schematic description of such a system.) Our goal is to characterize how the external driving (strong signal) affects propagation of another

wave (weak signal) propagating in the plasma channel in the xy -plane. For simplicity, we neglect gradients in the z direction, resulting in the linearized continuity equation (2). Time variation of ε may be attributed to the effect of the driving on the bound electrons of the ambient crystal. Our plasma is spatially homogeneous ($N_0(t)$ and $\varepsilon(t)$ are space-independent). Consequently, it is enough to consider waves with spatial dependence $\sim e^{i\mathbf{k}\cdot\mathbf{r}}$.

Owing to isotropy of our system, its excitations can be decoupled into longitudinal and transverse. Below we consider various examples of temporal modulation applied to longitudinal and transverse plasmons.

Longitudinal Plasmons. This class of waves is characterized by having $\mathbf{B} = 0$ and $\mathbf{E} = -\nabla\phi$, where ϕ is the electric potential. The potential ϕ and the charge density n obey the dynamic Poisson equation

$$\nabla \cdot \mathbf{E}(\mathbf{r}, t) \equiv -\nabla^2 \phi(\mathbf{r}, t) = \frac{4\pi e}{\varepsilon(t)} n(\mathbf{r}, t). \quad (4)$$

It is convenient to express the time-modulated quantities $N_0(t) = n_0(1 + \delta n(t))$ and $\varepsilon(t) = \varepsilon_0(1 + \delta\varepsilon(t))$ in terms of the fractional dimensionless functions $\delta n(t)$ and $\delta\varepsilon(t)$.

At this point, it is useful to introduce the scalar function $f(\mathbf{r}, t) = \nabla \cdot \mathbf{v}(\mathbf{r}, t)$. It then follows from Eqs.(2)-(4) that $f(\mathbf{r}, t)$ satisfies the second order equation

$$\frac{\partial^2 f}{\partial \tau^2} + \omega_p^2 \frac{\varepsilon(t)}{\varepsilon_0} (1 + \delta n(t)) f + \nu \frac{\partial}{\partial \tau} \left(\frac{\varepsilon(t)}{\varepsilon_0} f \right) = 0, \quad (5)$$

where similarly to the discussion of the parametric oscillator in³⁸ we introduced the new time variable $d\tau = dt \varepsilon_0 / \varepsilon(t)$. Furthermore, $\omega_p^2 = \frac{4\pi e^2 n_0}{m \varepsilon_0}$ is the (square of the) plasma frequency of the unmodulated (equilibrium) system.

If the modulation is such that $\varepsilon(t)$ never vanishes (so that transformation of the time variable is always regular), not much is lost by considering the simpler case of time-independent $\varepsilon = \varepsilon_0$ and avoiding this transformation altogether. In this case, we obtain

$$\frac{\partial^2 f}{\partial t^2} + \omega_p^2 (1 + \delta n(t)) f + \nu \frac{\partial f}{\partial t} = 0 \quad (6)$$

namely, the equation for a damped parametric oscillator³⁸. Note in passing that the first-order damping term in (6) may be eliminated by redefining $f = e^{-\nu t/2} g$. The resulting equation for g is

$$\frac{\partial^2 g}{\partial t^2} + \omega_p^2 \left(1 - \frac{\nu^2}{4\omega_p^2} + \delta n(t) \right) g = 0. \quad (7)$$

A unique feature of (5) and (6) is that they do not contain the wave number k . This is specific to *longitudinal* plasmons, due to their k -independent dispersion relation (in the absence of modulation) $\omega = \pm\omega_p$ (see the dashed lines in Fig 1a.) Such dispersion implies that after time modulation is switched on, exponential growth of f (and all other relevant quantities) becomes possible, simultaneously for *all* k -modes. This collective instability facilitates interaction of the plasma with the external driving circuitry, culminating in strong parametric amplification, as we explain in detail below.

The two Floquet-type fundamental solutions of (6) are of the form³⁹⁻⁴² $f_{1,2}(t) = e^{-i\omega_{1,2}t} u_{1,2}(t)$, where $\omega_{1,2}$ are the two fundamental frequencies, and $u_{1,2}(t)$ are periodic functions with period $T = 2\pi/\Omega$. Thus, $f_{1,2}(t+T) = e^{-i\omega_{1,2}T} f_{1,2}(t) = \Lambda_{1,2} f_{1,2}(t)$, where $\Lambda_{1,2} = e^{-i\omega_{1,2}T}$ are the eigenvalues of the temporal transfer matrix \mathbf{T} , which acts on the two dimensional space of solutions of (6) and propagates them through one period of time. The fundamental frequencies $\omega_{1,2} = \omega'_{1,2} + i\omega''_{1,2}$ are typically complex. Thus, if at least one of the imaginary parts $\omega''_{1,2}$ is negative, the corresponding eigenvalues $\Lambda_{1,2}$ will be larger than 1 in absolute values. Therefore, the corresponding Floquet solution will grow as function of time, rendering the system unstable.

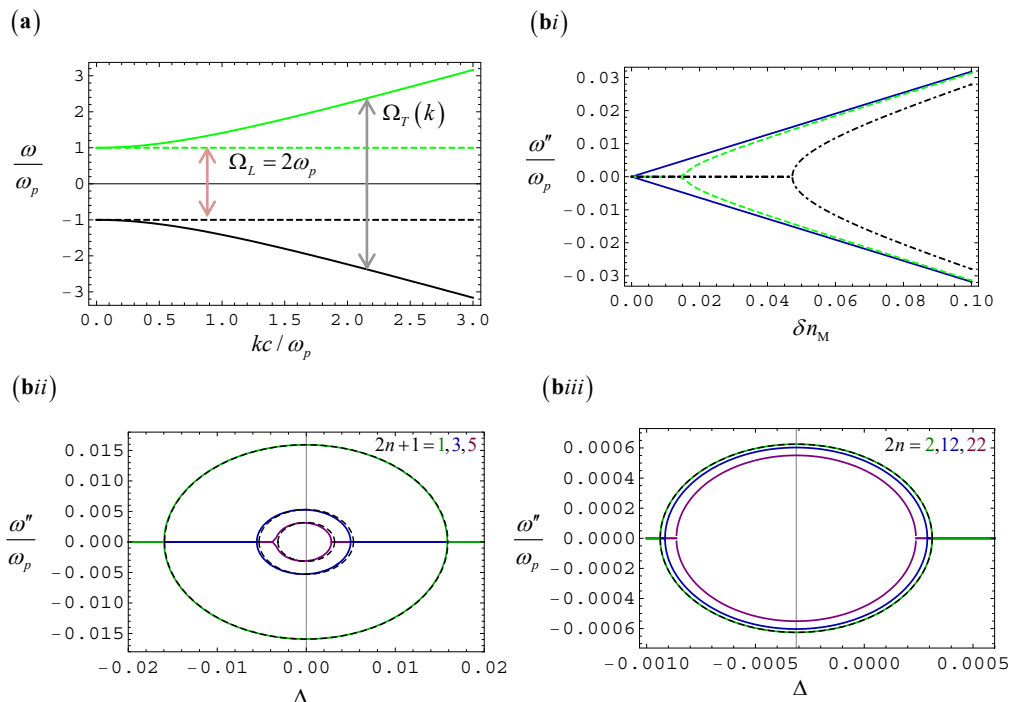


FIG. 1: **a)** Band structure of the static dispersive crystal, showing both positive and negative frequency bands. The arrows indicate possible interband transitions. **bi)** ω'' as a function of the (weak) modulation strength for i) $\Omega = 2\omega_p$ (blue solid lines), ii) $\Omega = (2 \pm 0.01)\omega_p$ (green dashed lines) and iii) $\Omega = (2 \pm 0.03)\omega_p$ (black dotted lines). **bii)** ω'' as a function of the detuning parameter Δ for fixed weak modulation amplitude $\delta n_M = 0.05$ for the first three odd resonances ($2n + 1 = 1, 3, 5$) in (11). The dashed curves are the analytic predictions. The three resonances are centered at $\Delta = 0$ and the growth rate becomes smaller as n increases. **biii)** The same as in **bii)** with $\delta n_M = 0.05$ for the even resonances $2n = 2, 12, 22$ in (12). Note the smaller vertical scale compared to the previous case. The three displayed resonances are in good agreement with the n -independent prediction of (12), despite the large disparity of chosen values for n . Evidently, these three resonances are centered around a negative value of Δ consistent with $-\delta n_M^2/8$ as predicted in (12).

The eigenvalues $\Lambda_{1,2}$ depend on the modulation frequency Ω and on the parameters controlling the (dimensionless) modulation profile $\delta n(t)$. This parameter space is split into regions of stability and instability, separated by borderlines. In regions of stability, oscillations of $f(t)$ are bounded, while in regions of instability $f(t)$ exhibits resonant behavior, with unbounded oscillations. See Section II of⁴² for more elementary details about Floquet theory.

These general statements about stability properties of (6) are demonstrated succinctly by the following two examples:

(i) *harmonic modulation*:

$$\delta n(t) = \delta n_M \cos \Omega t. \quad (8)$$

In this case (and in the absence of losses) Eq.(6) reduces to the famous Mathieu equation^{39–41,43,44}, which exhibits rich structure of stability and instability regions in the space of parameters Ω/ω_p and δn_M . In particular, for $\Omega = 2\omega_p$, it is well known that the amplitude of oscillations grows exponentially approximately as $\exp(\delta n_M \omega_p t/4)$. It is instructive to interpret this instability as a collective resonance (i.e., for all values of the wavenumber k) between the two branches $\pm\omega_p$ of the

static (unmodulated) crystal. This instability persists also when Ω is slightly detuned away from $2\omega_p$, albeit with a smaller growth exponent³⁸

$$\omega'' \simeq \frac{\omega_p}{4} \sqrt{\delta n_M^2 - 16\Delta^2} \quad (9)$$

where $\Delta = (\Omega/2\omega_p) - 1$ is the detuning parameter. The width of the instability region around $\Omega = 2\omega_p$ is determined by reality of ω'' . In particular, this means that there is a minimal threshold value of $\delta n_M^{\text{Th}} = 4|\Delta|$ required to induce instability. Similar but weaker instabilities occur also at modulation frequencies around $\Omega_n = 2\omega_p/n$ with integer n ³⁸. Finally, such exponential growth, albeit with smaller amplification rate $\omega''(\nu) \simeq \omega''(0) - \nu/2$, persists also for sufficiently small ν , as should be clear from the argument leading to (7)³⁸.

Note that in the same Fig.1a we also plotted the two branches of the spectrum for a transverse plasmon $\omega = \pm\omega(k)$, discussed in the next subsection. These spectral branches are sometimes referred to in the literature as “bands”, not to be confused with (time) Bloch bands, which appear only after periodic modulation is switched on^{3,4}.

(ii) *periodic piecewise constant modulation*: In this

case, in its simplest form, $\delta n(t)$ assumes one constant value δn_1 during the first part $0 \leq t < \tau$ of the modulation period and another constant value δn_2 during its remaining part $\tau \leq t < T^{39,40}$. The spatial analog of Eq. (7) with this type of modulation is the familiar Kronig-Penney model for energy band structure in one dimensional crystals.

For concreteness, let us focus on the modulation

$$\delta n(t) = \delta n_M \operatorname{sgn}(\sin(\Omega t)) \quad (10)$$

which flips sign at the middle of the modulation period. Here, as in the case of Mathieu's equation, one obtains a rich chart of stability and instability regions in the plane of parameters Ω/ω_p and δn_M ^{39,40}. In particular, for weak modulation amplitude δn_M (and in the absence of dissipation $\nu = 0$), one finds an infinite family of resonances analogous to the aforementioned resonance of the Mathieu equation, centered at modulation frequencies $\Omega_n^{\text{odd}} = 2\pi/T = 2\omega_p/(2n+1)$ with integer n , and with growth exponents⁴²

$$\omega'' = \omega_p \sqrt{\frac{\delta n_M^2}{((2n+1)\pi)^2} - \Delta^2}, \quad (11)$$

where $\Delta = \Omega/\Omega_n^{\text{odd}} - 1$ is the detuning parameter. Thus, at the center of the resonance ($\Delta = 0$), $\omega''_{\text{Res}} = \omega_p \delta n_M / (2n+1)\pi$ is linear in δn_M , and is therefore of leading order in perturbation theory. Furthermore, similarly to the corresponding result (9) for the Mathieu case (8), detuning the modulation frequency away from the resonance requires a threshold value $\delta n_M^{\text{Th}} = (2n+1)\pi|\Delta|$ of the modulation amplitude to induce instability with diminished ω'' .

In addition to this family of ‘linear’ resonances, we show in the Supplemental Material that there is yet another family of weaker resonances centered in the vicinity of modulation frequencies $\Omega_n^{\text{even}} = 2\omega_p/2n = \omega_p/n$ with integer n , with growth exponents

$$\omega'' = \omega_p \sqrt{\left(\frac{\delta n_M^2}{4}\right)^2 - \left(\Delta + \frac{\delta n_M^2}{8}\right)^2} \quad (12)$$

where $\Delta = \Omega/\Omega_n^{\text{even}} - 1$ is the detuning parameter away from Ω_n^{even} . In contrast with (11), the centers of these resonances (i.e., maximal instability) occur at modulation frequencies $\Omega_n^{\text{Res}} = \Omega_n^{\text{even}}(1 - \delta n_M^2/8)$, which depend quadratically on δn_M . Furthermore, at $\Omega = \Omega_n^{\text{Res}}$, all these resonances share an n -independent common growth exponent $\omega''_{\text{Res}} = \omega_p \delta n_M^2/4$, quadratic in δn_M , and therefore of higher order in perturbation theory.

The predictions of (11) and (12) are compared against numerical simulation of the piecewise constant modulation in Fig.1bi-iii, showing excellent agreement.

For completeness, in Fig.2 we show numerical results for the growth rates ω'' of resonances arising at fixed

strong modulation amplitude $\delta n_M = 0.5$ as function of the modulation frequency Ω . The general pattern of resonances at weak modulation amplitudes, summarized in (11) and (12), is clearly preserved, up to some amount of bounded shifts in resonance frequencies. However, as can be clearly seen in Fig.2, at strong modulation amplitude, the strength of the even resonances of (12) can become comparable, or even surpass the odd resonances of (11).

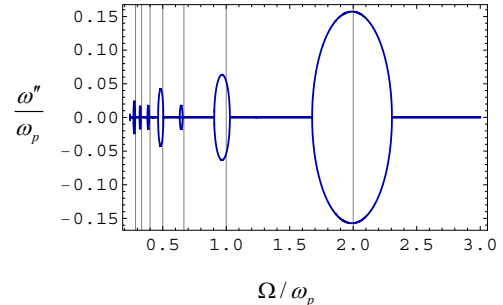


FIG. 2: ω'' as a function of the modulation frequency Ω for fixed *strong* modulation amplitude $\delta n_M = 0.5$. The vertical grid lines mark the modulation frequencies $\Omega = 2\omega_p/m$ with $m = 1, 2, \dots, 7$ at the positions of the linear (odd m) and quadratic (even m) resonances (Eqs.(11) and (12), respectively) in the case of weak modulation amplitude.

In the Supplementary Material we give a simple perturbative derivation of the growth rate ω'' of ‘linear resonances’ (at zero detuning $\Delta = 0$ and in the absence of losses $\nu = 0$) for an arbitrary weak periodic modulation profile $\delta n(t)$ in (6), which includes (9) and (11) as special cases. To this end consider the Fourier decomposition $\delta n(t) = \sum_{l=1}^{\infty} (c_l \exp(i l \Omega t) + c_l^* \exp(-i l \Omega t))$ of the modulation amplitude. Resonant behavior of $f(t)$ should be expected when the modulation frequency Ω is commensurate with the gap $2\omega_p$ in the dispersion relation of the unmodulated longitudinal plasmon, such that $2\omega_p/\Omega = n$, with integer n . In this case, the n th Fourier mode of $\delta n(t)$ will become resonant, and will induce instability with growth rate

$$\omega'' = \frac{\omega_p |c_n|}{2}. \quad (13)$$

This result is linear in c_n , and therefore in δn , being the result of first order perturbation theory.

For example, in the Mathieu case (8), $c_l = (\delta n_M/2)\delta_{l,1}$, so there is only one linear resonance which occurs for $n = 1$ at $\Omega = 2\omega_p$ and with the known growth exponent $\omega'' = \omega_p \delta n_M/4$.

For the piecewise constant modulation (10), all even Fourier modes $c_{2n} = 0$ vanish, while the odd ones are $c_{2n+1} = 2\delta n_M/(2n+1)\pi i$. Thus, there is an *infinite set of linear resonances* at modulation frequencies $\Omega = 2\omega_p/(2n+1)$, with corresponding growth exponents $\omega'' = \omega_p \delta n_M/(2n+1)\pi$, which agrees with the aforementioned result (11). In this case, there are no *linear* resonances corresponding to even index $2n$ simply because

there are no Fourier modes of even order in the modulation (10). Finally, as we mention in⁴², modulation by a comb of Dirac-delta impulses can be realized as a certain limit of piecewise constant modulation. Such modulation induces ‘linear’ resonances, whose growth rates are given by our general formula (13) in the limit of weak modulation amplitude.

Transverse Plasmons. We shall now briefly consider temporal modulation of transverse plasmons^{18,32–36}, mainly in order to compare it against that of longitudinal plasmons. For simplicity, we shall assume in this section that the material dissipation is negligible ($\nu = 0$). Transverse waves are governed by the two Maxwell equations (1), the (linearized) continuity equation (2), and by Newton’s law for electrons (3). (The two remaining Maxwell equations, namely, Gauss’ law (4) for the electric field and solenoidality $\nabla \cdot \mathbf{B}(\mathbf{r}, t) = 0$ of the magnetic field, need only be imposed at the initial time of evolution, and automatically persist at later times.) Since the medium in question is translationally invariant, it is enough to consider plane-wave solutions $\sim e^{i\mathbf{k} \cdot \mathbf{r}}$, and analyze the dynamics of a wave with a fixed wave-vector \mathbf{k} . (In order to avoid notational cluttering, we shall omit the Fourier index k from all relevant physical quantities.)

Due to isotropy of the medium, with no loss of generality, henceforth we take $\mathbf{E} = E\hat{\mathbf{z}}, \mathbf{B} = B\hat{\mathbf{y}}, \mathbf{k} = k\hat{\mathbf{x}}$ and $\mathbf{v} = v\hat{\mathbf{z}}$. Thus, $\mathbf{j} = eN_0(t)\mathbf{v} \perp \mathbf{k}$, leading to $\partial n/\partial t = -i\mathbf{k} \cdot \mathbf{j} = 0$ from (2). This ensures consistency of (the time derivative of) Eq. (4) and the second equation in (1). After substituting our Ansatz, Eqs. (1) and (3) reduce to

$$\begin{aligned} \frac{\partial v}{\partial t} &= \frac{e}{m}E, & \frac{\partial B}{\partial t} &= ikcE \\ \frac{\partial}{\partial t} [\varepsilon(t)E] &= ikcB - 4\pi j \text{ with } j = eN_0(t)v. \end{aligned} \quad (14)$$

Note that if we set $N_0(t) = 0$ in the above equations (no free electrons), but allow temporal modulation of the term $\varepsilon(t)$, we recover the dynamic equations for a standard photonic crystal in a temporally modulated dielectric.

It is convenient at this point to derive a second order differential equation for B rather than for E , in order to avoid the necessity of taking a time derivative of $N_0(t)$. To this end, we first eliminate $v = \frac{-ie}{ckm}B$ from the first pair of equations in (14) and use this result to express j in terms of B . Then, by taking the time derivative of the second equation in (14), with the use of the equation for j following it, we obtain our desired equation for B as $\frac{\partial}{\partial t} (\varepsilon(t) \frac{\partial B}{\partial t}) + \left(k^2 c^2 + \frac{4\pi N_0(t) e^2}{m} \right) B = 0$.

Assuming that $\varepsilon = \varepsilon_0$ is time-independent, it is straightforward to show that B satisfies

$$\frac{d^2 B}{dt^2} + \omega_T^2 \left[1 + \frac{\omega_p^2}{\omega_T^2} \delta n(t) \right] B = 0, \quad (15)$$

where $\omega_T^2 = \frac{c^2 k^2}{\varepsilon_0} + \omega_p^2$ is the transverse plasmon frequency, for a given wavenumber k . Equation (15) is sim-

ilar in form to (6) (with $\nu = 0$), coincides with the latter at $k = 0$, and therefore describes a parametric oscillator, as in the case of longitudinal plasmons. Evidently, we can translate the entire previous discussion of resonances in modulated longitudinal plasmons to transverse plasmons, simply by replacing ω_p in the appropriate places by ω_T and by rescaling the modulation amplitude $\delta n(t)$ by a factor ω_p^2/ω_T^2 . Thus, compared to the longitudinal case, the modulation amplitude is effectively reduced and the resonance frequency of the system is increased. Stability regions in the parameter space pertaining to modulated longitudinal plasmons become k -bands of the transverse PLTC, while regions of instability correspond to gaps.

We stress that the resonances associated with (15) arise for each wavenumber k separately, in contrast with the collective, k -independent nature of resonances in modulated longitudinal plasmons.

For example, in the case of piecewise constant modulation (10), we see from (11) pertaining to longitudinal plasmons, that there will be resonances of the transverse plasmon at modulation frequency $\Omega_{n,T}^{\text{odd}} = 2\omega_T/(2n+1)$ with integer n and growth exponents $\omega'' = \omega_T \sqrt{(\omega_p^2 \delta n_M / (2n+1) \pi \omega_T^2)^2 - \Delta^2}$, in which $\Delta = \Omega/\Omega_{n,T}^{\text{odd}} - 1$ is the detuning parameter. Analogous results exist obviously also for the weaker longitudinal resonances (12).

Conclusions. In this Letter we carried a comprehensive study of *plasmonic time crystals*, demonstrating that these platforms support both longitudinal and transverse modes. We have shown that under a periodic time modulation, these systems function as parametric oscillators. We have analyzed their stability properties across various parameters. Notably, the resonance of the longitudinal modes does not depend on the wave vector \mathbf{k} , allowing these modes to undergo a collective resonance. This characteristic can be leveraged to achieve optical amplification.

In contrast, transverse PLTCs depend on the \mathbf{k} -vector of propagating waves, and in this case, stability regions in parameter space correspond to k -bands of the PLTC, while instability regions correspond to gaps. The strongest parametric instabilities are determined by interband transitions at modulation frequency $\Omega = 2\omega_T$. Higher-order instabilities result from related mechanisms but at lower modulation rates.

Remarkably, we find that for piecewise modulation there is an infinite family of resonances with common growth rate associated with modulation frequencies that scale as $2\omega_p/n$ ($2\omega_T/n$) for longitudinal (transverse) plasmons, with even index n .

Acknowledgments

JF is supported in part by grant No.2022158 from the United States - Israel Binational Science Foundation (BSF), Jerusalem, Israel. D.E.F. acknowledges financial

support by IT-Lisbon and FCT under a research contract Ref. CEECINST/00058/2021/CP2816/CT0003 and DOI identifier <https://doi.org/10.54499/CEECINST/00058/2021/CP2816/CT0003>. BS is indebted to Remi Carminati for useful discussions at the early stage of this work. MS is partially supported by the IET, by the Simons Foundation under the award 733700

(Simons Collaboration in Mathematics and Physics, “Harnessing Universal Symmetry Concepts for Extreme Wave Phenomena”), by Fundação para a Ciência e a Tecnologia and Instituto de Telecomunicações under projects UIDB/50008/2020 and DOI identifier <https://doi.org/10.54499/UIDB/50008/2020> and 2022.06797.PTDC.

-
- ¹ C. Caloz and Z.-L. Deck-Léger, *Spacetime metamaterials - Part I: General concepts*, IEEE Trans. Antennas Propag. **68**, 1569 (2020); *Spacetime metamaterials - Part II: Theory and Applications*, IEEE Trans. Antennas Propag. **68**, 1583 (2020).
- ² E. Galiffi, R. Tirole, S. Yin, H. Li, S. Vezzoli, P. A. Huidobro, M.G. Silveirinha, R. Sapienza, A. Alù, and J. B. Pendry, *Photonics of time-varying media*, Adv. Photon. **4**, 014002 (2022).
- ³ Y. Sharabi, E. Lustig, and M. Segev, *Disordered Photonic Time Crystals*, Phys. Rev. Lett. **126**, 163902 (2021).
- ⁴ J. R. Zurita-Sánchez, P. Halevi, and J. C. Cervantes-González, *Reflection and transmission of a wave incident on a slab with a time-periodic dielectric function*, Phys. Rev. A **79**, 053821 (2009).
- ⁵ F. Morgenthaler, *Velocity modulation of electromagnetic waves*, IRE Trans. Microw. Theory Tech. **6**, 167 (1958).
- ⁶ R. Carminati, H. Chen, R. Pierrat, and B. Shapiro, *Universal Statistics of Waves in a Random Time-Varying Medium*, Phys. Rev. Lett. **127**, 094101 (2021).
- ⁷ A. Akbarzadeh, N. Chamanara, and C. Caloz, *Inverse prism based on temporal discontinuity and spatial dispersion*, Opt. Lett. **43**, 3297 (2018).
- ⁸ V. Pacheco-Peña and N. Engheta, *Temporal aiming*, Light Sci. Appl. **9**, 129 (2020).
- ⁹ J. Xu, W. Mai, and D. H. Werner, *Complete polarization conversion using anisotropic temporal slabs*, Opt. Lett. **46**, 1373 (2021).
- ¹⁰ H. Li, S. Yin, E. Galiffi, and A. Alù, *Temporal Parity-Time Symmetry for Extreme Energy Transformations*, Phys. Rev. Lett. **127**, 153903 (2021).
- ¹¹ H. Li, S. Yin, and A. Alù, *Nonreciprocity and Faraday Rotation at Time Interfaces*, Phys. Rev. Lett. **128**, 173901 (2022).
- ¹² A. Dikopoltsev, Y. Sharabi, M. Lyubarov, Y. Lumer, S. Tsesses, E. Lustig, I. Kaminer, and M. Segev, *Light emission by free electrons in photonic time-crystals*, Proc. Natl. Acad. Sci. USA **119**, e2119705119 (2021).
- ¹³ N. V. Budko, *Electromagnetic radiation in a time-varying background medium*, Phys. Rev. A **80**, 053817 (2009).
- ¹⁴ M. Lyubarov, Y. Lumer, A. Dikopoltsev, E. Lustig, Y. Sharabi, and M. Segev, *Amplified emission and lasing in photonic time crystals*, Science **377**, 425 (2022).
- ¹⁵ E. Lustig, Y. Sharabi, and M. Segev, *Topological aspects of photonic time crystals*, Optica **5**, 1390 (2018).
- ¹⁶ M. J. Mencagli, D. L. Sounas, M. Fink, and N. Engheta, *Static-to-dynamic field conversion with time-varying media*, Phys. Rev. B **105**, 144301 (2022).
- ¹⁷ H. Li, S. Yin, H. He, J. Xu, A. Alù and B. Shapiro, *Stationary Charge Radiation in Anisotropic Photonic Time Crystals*, Phys. Rev. Lett. **130**, 093803 (2023).
- ¹⁸ D. M. Solís, R. Kastner, and N. Engheta, *Time-varying materials in the presence of dispersion: Plane-wave propagation in a Lorentzian medium with temporal discontinuity*, Photon. Res. **9**, 1842 (2021).
- ¹⁹ D. M. Solís and N. Engheta, *Functional analysis of the polarization response in linear time-varying media: A generalization of the Kramers-Kronig relations*, Phys. Rev. B **103**, 144303 (2021).
- ²⁰ Z. Hayran, J. B. Khurgin, F. Monticone, *$\hbar\omega$ versus $\hbar k$: dispersion and energy constraints on time-varying photonic materials and time crystals*, Optics Material Express, **12** 3904, (2022).
- ²¹ J. Sloan, N. Rivera, J. D. Joannopoulos, and M. Soljacic, *Optical Properties of Dispersive Time-Dependent Materials*, ACS Photonics, **11**, 950, (2024).
- ²² S. A. R. Horsley, E. Galiffi and Y.-T. Wang, *Eigenpulses of Dispersive Time-Varying Media*, Phys. Rev. Lett. **130**, 203803, (2023).
- ²³ G. Ptitsyn, A. Lampranidis, T. Karamanos, V. Asadchy, R. Alaee, M. Müller, M. Albooyeh, M. Sajjad Mirmoosa, S. Fan, S. Tretyakov and C. Rockstuhl, *Floquet-Mie Theory for Time-Varying Dispersive Spheres*, Laser Photonics Rev. **17**, 2100683 (2022).
- ²⁴ M. M. Dimitrijevic and B. V. Stanic, *EMW Transformation in Suddenly Created Two-Component Magnetized Plasma*, IEEE Trans. Plasma Sci. **23**, 422, (1995).
- ²⁵ D. Holberg and K. Kunz, *Parametric properties of fields in a slab of time-varying permittivity*, IEEE Trans. Antennas Propag., **14**, 183, 1966.
- ²⁶ F. R. Prudêncio and M. G. Silveirinha, *Synthetic Axion Response with Spacetime Crystals*, Phys. Rev. Appl. **19**, 024031, (2023).
- ²⁷ F. R. Prudêncio and M. G. Silveirinha, *Replicating Physical Motion with Minkowskian Isorefractive Spacetime Crystals*, Nanophotonics, 10.1515/nanoph-2023-0144, (2023).
- ²⁸ V. Bacot, M. Labousse, A. Eddi, M. Fink, and E. Fort, *Time reversal and holography with spacetime transformations*, Nat. Phys. **12**, 972 (2016).
- ²⁹ V. Bacot, G. Durey, A. Eddi, M. Fink, and E. Fort, *Phase-conjugate mirror for water waves driven by the Faraday instability*, Proc. Natl. Acad. Sci. U. S. A. **116**, 8809 (2019).
- ³⁰ H. Moussa, G. Xu, S. Yin, E. Galiffi, Y. Radi, and A. Alù, *Observation of Temporal Reflections and Broadband Frequency Translations at Photonic Time-Interfaces*, Nat. Phys. **19**, 863 (2023).
- ³¹ B. Appfel, S. Wildeman, A. Eddi, and E. Fort, *Experimental Implementation of Wave Propagation in Disordered Time-Varying Media*, Phys. Rev. Lett. **128**, 094503 (2022).
- ³² H. He, S. Zhang, J. Qi, F. Bo, and H. Li, *Faraday rotation in nonreciprocal photonic time-crystals*, Appl. Phys. Lett. **122**, 051703 (2023).
- ³³ J. C. Serra, M. G. Silveirinha, *Homogenization of Dispersive Spacetime Crystals: Anomalous Dispersion and Neg-*

- ative Stored Energy, Phys. Rev. B **108**, 035119, (2023).
- ³⁴ J. C. Serra, E. Galiffi, P. A. Huidobro, J. B. Pendry and M. G. Silveirinha, *Particle-hole instabilities in photonic time-varying systems*, Opt. Mat. Express, **14**, 1459, (2024). (arXiv:2402.08507).
- ³⁵ F. Feng, N. Wang, G. P. Wang, *Temporal transfer matrix method for Lorentzian dispersive time-varying media*, Appl. Phys. Lett. **124**, 101701 (2024).
- ³⁶ K-H. Kim and K-H. O, *Graphene Plasmonic Time Crystals*, Physica Status Solidi (rapid research letters) **2024**, 2400116.
- ³⁷ S. Zhang, J. Dong, H. Li, J. Xu and B. Shapiro, *Longitudinal optical phonons in stationary charge-embedded photonic time crystals*, arXiv:2407.04502 (2024).
- ³⁸ L. D. Landau and E. M. Lifshitz, *Mechanics*, 3rd edition, (Pergamon Press, Oxford, 1976), section 27.
- ³⁹ L. Brillouin, *Wave Propagation in Periodic Structures - Electric Filters and Crystal Lattices*, (McGraw Hill Book Company, New York, 1946), Chapter 8.
- ⁴⁰ B. van der Pol and M. J. O. Strutt, *On the Stability of the Solutions of Mathieu's Equation*, Phil. Mag. **5** 18 (1928).
- ⁴¹ W. Magnus and S. Winkler, *Hill's Equation*, (Dover Publications, New York, 2004).
- ⁴² See the Supplementary Material for this Letter for more details.
- ⁴³ F. M. Arscott, *Periodic Differential Equations*, (The MacMillan Company, New York, 1964), Chapter 6. D. W. Jordan and P. Smith, *Nonlinear Ordinary Differential Equations*, 4th edition, (Oxford University Press, Oxford, 2007), Chapter 9.
- ⁴⁴ I. Kiorpelidis, F. K. Diakonov, G. Theocharis, and V. Pagneux, *Transient amplification in Floquet media: the Mathieu oscillator example*, arXiv:2404.00138 (2024).

Supplementary Material for ‘Plasmonic Time Crystals’

Joshua Feinberg*

Department of Physics and Haifa Center for Physics and Astrophysics,
University of Haifa, Haifa 3498838, Israel

David E. Fernandes

University of Lisbon and Instituto de Telecomunicações ,
Avenida Rovisco Pais 1, Lisboa, 1049-001, Portugal

Boris Shapiro

Department of Physics
Technion, Israel Institute of Technology, Haifa 32000, Israel

Mário G. Silveirinha

University of Lisbon and Instituto de Telecomunicações,
Avenida Rovisco Pais 1, Lisboa, 1049-001, Portugal

(Dated: July 30, 2024)

I. SCHEMATIC DESCRIPTION OF THE REALIZATION OF THE PLASMONIC SYSTEM

A possible realization of plasma with time-varying N_0 is depicted in Fig. S1. An electronic “pump” creates a time-varying oscillating current along the z -direction ($\mathbf{J}_0 \sim \hat{\mathbf{z}}$), inducing time variation of N_0 .

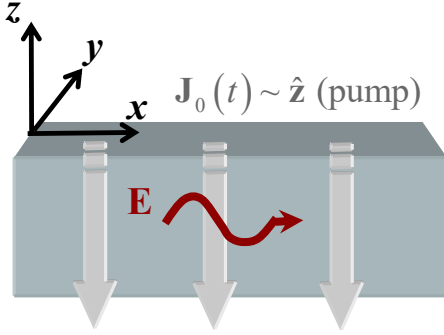


FIG. S1: Illustration of the plasmonic time crystal: the figure depicts the process of electronic carrier injection/removal via a time-varying current directed along the z -axis symbolized by the gray arrows (pump, i.e., the strong signal). The temporal modulation tailors the propagation of a weak signal traversing the plasma channel in the xy -plane.

II. SUMMARY OF RELEVANT RESULTS FROM FLOQUET THEORY

For concreteness we refer to Equations (6) and (7) in the main text:

$$\frac{\partial^2 f}{\partial t^2} + \omega_p^2(1 + \delta n(t))f + \nu \frac{\partial f}{\partial t} = 0 \quad (1)$$

and

$$\frac{\partial^2 g}{\partial t^2} + \omega_p^2 \left(1 - \frac{\nu^2}{4\omega_p^2} + \delta n(t) \right) g = 0, \quad (2)$$

where $f = e^{-\nu t/2}g$.

The two Floquet-type fundamental solutions of (1) are of the form¹⁻³ $f_{1,2}(t) = e^{-i\omega_{1,2}t}u_{1,2}(t)$, where $\omega_{1,2}$ are the two fundamental frequencies, and $u_{1,2}(t)$ are periodic functions with period $T = 2\pi/\Omega$. Thus, $f_{1,2}(t+T) = e^{-i\omega_{1,2}T}f_{1,2}(t) = \Lambda_{1,2}f_{1,2}(t)$, where $\Lambda_{1,2} = e^{-i\omega_{1,2}T}$ are the eigenvalues of the temporal transfer matrix \mathbf{T} , which acts on the two dimensional space of solutions of (1) and propagates them through one period of time. By studying the Wronskian $W(f_1, f_2)$ one can show that $\Lambda_1\Lambda_2 = e^{-\nu T}$, or equivalently, $\omega_1 + \omega_2 = -i\nu + n\Omega$ with integer n .

The coefficient functions in (1) are all real, so that if f is a solution, so is f^* . Thus, there are two possibilities: either (i) $f_2(t) = f_1^*(t)$, or (ii) $f_1(t)$ and $f_2(t)$ are both real. Case (i) corresponds to *stable oscillations*, for which $\Lambda_2 = \Lambda_1^*$, so that $|\Lambda_1|^2 = e^{-\nu T} \leq 1$. Therefore, both $f_{1,2}(t)$ are bounded and the system is stable. In this case $e^{i(\omega_1^* + \omega_2)T} = 1$ so that we can always choose $\omega_{1,2} = \pm\omega' - i\nu/2$. In contrast to case (i), case (ii) typically corresponds to *unstable oscillations*, where both Λ_1 and Λ_2 are real and of the same sign. For $\nu = 0$, one of them must be larger than 1 in absolute value. In this case, one of the solutions becomes unbounded at large times,

*<https://orcid.org/0000-0002-2869-0010>

rendering the system unstable. By continuity this instability should also persist after ν is turned on, for small enough values of ν . If both $\Lambda_1, \Lambda_2 > 0$ then $\omega_1 = i\omega''$ and $\omega_2 = -i(\omega'' + \nu)$ are pure imaginary. Alternatively, if both $\Lambda_{1,2}$ are negative, then $e^{-i\omega_{1,2}T} = \Lambda_{1,2} = |\Lambda_{1,2}|e^{\pm i\pi}$ so that $\text{Re } \omega_{1,2} = \omega'_{1,2} = \pm\pi/T = \pm\Omega/2$ (as is evident for example from the numerical results plotted in Fig.1biii in the main text.)

III. PIECEWISE CONSTANT MODULATION

A. Modulation Period with Two Different Amplitude Values

Here we shall derive equations (11) and (12) of the main text - the expressions for the growth exponents associated with resonances of odd and even indices, respectively. In the next subsection we shall also solve this model in the limit in which the piecewise modulation becomes a time-periodic Dirac comb of δ -impulses.

In the simplest form of piecewise constant periodic modulation, $\delta n(t)$ assumes one constant value δn_1 during the first part $0 \leq t < \tau$ of the modulation period and another constant value δn_2 during its remaining part $\tau \leq t < T^{1,2}$.

The common practice to solving (2) with periodic modulation is to analyze the initial value problem, and compute the two independent fundamental solutions $c(t)$ and $s(t)$ with initial conditions $c(0) = 1; \dot{c}(0) = 0$ and $s(0) = 0; \dot{s}(0) = 1$ (namely, the cosine- and sine-like solutions). These solutions can be easily computed explicitly in our case of piecewise constant modulation. The transfer matrix \mathbf{T} is then constructed from the values of these fundamental solutions and their derivatives at $t = T^3$. Here we shall follow an alternative method⁴⁻⁶ (familiar from the theory of Lyapunov stability) to computing \mathbf{T} , but in a basis different from that of $\{c(t), s(t)\}$. (The eigenvalues $\Lambda_{1,2}$ of \mathbf{T} are of course basis independent.) To this end, we adopt a ‘‘hamiltonian’’ approach and rewrite (2) as a system of two coupled first order equations

$$\frac{d}{dt} \begin{pmatrix} \psi_1 \\ \psi_2 \end{pmatrix} = \begin{pmatrix} 0 & \omega_p \\ -\omega_p \left(1 - \frac{\nu^2}{4\omega_p^2} + \delta n(t)\right) & 0 \end{pmatrix} \begin{pmatrix} \psi_1 \\ \psi_2 \end{pmatrix} \quad (3)$$

with $\psi_1 = \omega_p g(t)$ and $\psi_2 = \dot{g}(t)$ (thus rendering ψ_1 and ψ_2 the same physical dimension). Equation (3) can be integrated formally by applying the time ordered exponent $\mathbf{U}(t, t_0) = \mathcal{T} \exp \left(\int_{t_0}^t \mathbf{L}(t') dt' \right)$ of the matrix $\mathbf{L}(t)$ (the ‘‘Liouvillian’’) on the right hand side of (3) to the vector of initial conditions at $t = t_0$. For constant δn , as in each part of the modulation period in the present example,

one can exponentiate \mathbf{L} explicitly and find

$$\mathbf{M}(\Theta; t) = e^{\mathbf{L}t} = \begin{pmatrix} \cos \Theta t & \frac{\omega_p}{\Theta} \sin \Theta t \\ -\frac{\Theta}{\omega_p} \sin \Theta t & \cos \Theta t \end{pmatrix} \quad (4)$$

with $\Theta = \omega_p \sqrt{1 - \frac{\nu^2}{4\omega_p^2} + \delta n}$. In the main text we focus on the modulation

$$\delta n(t) = \delta n_M \text{sgn}(\sin(\Omega t)) \quad (5)$$

which flips sign at the middle of the modulation period. In this case the transfer matrix for Eq.(2) is readily found as $\mathbf{T}_g = \mathbf{U}(T, 0) = \mathbf{M}(\Theta_-; T/2)\mathbf{M}(\Theta_+; T/2)$, where $\Theta_{\pm} = \omega_p \sqrt{1 - \frac{\nu^2}{4\omega_p^2} \pm \delta n_M}$.

From the relation $f = e^{-\nu t/2} g$ we have $(\omega_p f(t), \dot{f}(t))^T = e^{-\nu t/2} \mathbf{K}(\omega_p g(t), \dot{g}(t))^T$ with $\mathbf{K} = \begin{pmatrix} 1 & 0 \\ -\nu/2\omega_p & 1 \end{pmatrix}$, and therefore the transfer matrix for Eq. (1) is $\mathbf{T}_f = e^{-\nu T/2} \mathbf{K} \mathbf{T}_g \mathbf{K}^{-1}$. Thus,

$$\begin{aligned} \frac{1}{2} \text{Tr } \mathbf{T}_f &= \frac{1}{2} (\Lambda_1 + \Lambda_2) = \frac{1}{2} e^{-\nu T/2} \text{Tr } \mathbf{T}_g \\ &= e^{-\nu T/2} \left[\cos \left(\frac{\pi \Theta_+}{\Omega} \right) \cos \left(\frac{\pi \Theta_-}{\Omega} \right) \right. \\ &\quad \left. - \frac{1}{2} \left(\frac{\Theta_+}{\Theta_-} + \frac{\Theta_-}{\Theta_+} \right) \sin \left(\frac{\pi \Theta_+}{\Omega} \right) \sin \left(\frac{\pi \Theta_-}{\Omega} \right) \right] \quad (6) \end{aligned}$$

which coincides with the known result^{1,2} in the absence of dissipation $\nu = 0$. (See also chapter 8 of³ and note the obvious typo in Eq.(8.5) therein.)

For simplicity, from now on we shall focus on the non-dissipative case $\nu = 0$, and rewrite (6) more neatly as

$$\begin{aligned} \frac{1}{2} \text{Tr } \mathbf{T}_f &= \cos \left(\frac{\pi(\Theta_+ + \Theta_-)}{\Omega} \right) \\ &\quad - \frac{(\Theta_+ - \Theta_-)^2}{4\Theta_+\Theta_-} \cdot \left[\cos \left(\frac{\pi(\Theta_+ - \Theta_-)}{\Omega} \right) \right. \\ &\quad \left. - \cos \left(\frac{\pi(\Theta_+ + \Theta_-)}{\Omega} \right) \right]. \quad (7) \end{aligned}$$

In regions of stability, where $\Lambda_2^* = \Lambda_1 = e^{-i\omega T}$ (with real ω), we thus have $\frac{1}{2} \text{Tr } \mathbf{T}_f = \cos \omega T$, so that $|\text{Tr } \mathbf{T}_f/2| < 1$. In contrast, in the unstable regime we can always choose $\Lambda_1 = 1/\Lambda_2 = \pm e^{\omega'' T}$ with $\omega'' > 0$. Thus, $\omega = i\omega''$ for positive $\Lambda_{1,2}$, or $\omega = \pi/T + i\omega''$ for negative $\Lambda_{1,2}$ (where $\omega' = \pi/T$ is restricted to the first Brillouin zone). Therefore, in the unstable regime we have $\frac{1}{2} \text{Tr } \mathbf{T}_f = \pm \cosh(\omega'' T)$ so that $|\text{Tr } \mathbf{T}_f/2| > 1$. The boundaries separating stable and unstable regions are therefore given by the curves where $\text{Tr } \mathbf{T}_f/2 = \pm 1$. This leads, like in the case of Mathieu’s equation, to a rich chart of stability and instability regions in the plane of parameters Ω/ω_p and $\delta n_M^{1,2}$.

Let us now investigate the stability of this system perturbatively for weak modulation amplitude δn_M . In

this case, the factor $(\Theta_+ - \Theta_-)^2/\Theta_+\Theta_-$ in the second term in (7) is clearly of order δn_M^2 . Thus, the modulation frequencies which induce instabilities at infinitesimal $\delta n_M \rightarrow 0^+$ are determined in this limit by the leading term $\cos(\pi(\Theta_+ + \Theta_-)/\Omega) \simeq \cos(2\pi\omega_p/\Omega)$ in (7) tending to ± 1 . The first few terms of the expansion of (7) around $\delta n_M = 0$ are

$$\begin{aligned} \frac{1}{2}\text{Tr}\mathbf{T}_f &= \cos\left(\frac{2\pi\omega_p}{\Omega}\right) + \\ \frac{1}{2}\left[\frac{\pi\omega_p}{2\Omega}\sin\left(\frac{2\pi\omega_p}{\Omega}\right) - \sin^2\left(\frac{\pi\omega_p}{\Omega}\right)\right]\delta n_M^2 &+ \\ \frac{1}{32}\left[4\left(\frac{\pi\omega_p}{\Omega}\right)^2 - 6 + \left(6 - \left(\frac{\pi\omega_p}{\Omega}\right)^2\right)\cos\left(\frac{2\pi\omega_p}{\Omega}\right) + \right. \\ \left. \frac{9}{2}\frac{\pi\omega_p}{\Omega}\sin\left(\frac{2\pi\omega_p}{\Omega}\right)\right]\delta n_M^4 &+ \mathcal{O}(\delta n_M^6). \end{aligned} \quad (8)$$

The instability near $\cos(2\pi\omega_p/\Omega) = -1$ occurs around modulation frequencies $\Omega = 2\pi/T = 2\omega_p/(2n+1)$ with integer n . (In the expansion of (7) around $\delta n_M = 0$ leading to (8), we tacitly assumed T was bounded, which means that the integer n , indexing the corresponding parametric resonance, is assumed to be bounded as well.) Thus, let us substitute $\Omega = 2\omega_p(1+\Delta)/(2n+1)$ in (8), with Δ a small detuning parameter. We find $1/2\text{Tr}\mathbf{T}_f \equiv \cos((\omega' + i\omega'')T) = -1 - [\delta n_M^2 - (2n+1)^2\pi^2\Delta^2]/2 + \mathcal{O}(\delta n_M^2\Delta, \Delta^3) \simeq \cos\left(i\sqrt{\delta n_M^2 - (2n+1)^2\pi^2\Delta^2} \pm \pi\right)$. Therefore, up to the indicated accuracy, $\omega' = \pm\pi/T = \pm\omega_p(1+\Delta)/(2n+1)$ and

$$\omega'' = \omega_p\sqrt{\frac{\delta n_M^2}{((2n+1)\pi)^2} - \Delta^2}. \quad (9)$$

Thus, maximal instability (the center of the resonance) occurs at $\Delta = 0$, where $\omega''_{\text{Res}} = \omega_p\delta n_M/(2n+1)\pi$ is linear in δn_M , and is therefore of leading order in perturbation theory. Furthermore, similarly to the corresponding result for the Mathieu case, given in Eq. (9) in the main text, detuning the modulation frequency away from the resonance requires a threshold value $\delta n_M^{\text{Th}} = (2n+1)\pi|\Delta|$ of the modulation amplitude to induce instability with diminished ω'' .

This is not the case for the parametric resonances around the other instability borderline at $\cos(2\pi\omega_p/\Omega) = +1$, which occur in the vicinity of modulation frequencies $\Omega = 2\omega_p/2n = \omega_p/n$ with integer n . By substituting $\Omega = \omega_p(1+\Delta)/n$ in (8) and expanding the resulting expression in powers of Δ , we find that the associated resonance lies in the parametric regime where Δ scales like δn_M^2 so that $1/2\text{Tr}\mathbf{T}_f \equiv \cos((\omega' + i\omega'')T) = 1 + (1/2)(2\pi n)^2[\delta n_M^4/16 - (\Delta + \delta n_M^2/8)^2] + \mathcal{O}(\Delta^3, \delta n_M^2\Delta^2, \delta n_M^4\Delta, \delta n_M^6) \simeq \cosh\left[(2\pi n)\sqrt{\delta n_M^4/16 - (\Delta + \delta n_M^2/8)^2}\right]$. Thus, up to

the indicated accuracy

$$\omega'' = \omega_p\sqrt{\left(\frac{\delta n_M^2}{4}\right)^2 - \left(\Delta + \frac{\delta n_M^2}{8}\right)^2} \quad (10)$$

(and of course $\omega' = 0$). Thus, in contrast with (9), these resonances (that is, maximal instability) are not centered at modulation frequency $\Omega = \omega_p/n$ where $\cos(\omega T) = 1$ reaches the upper border of the stability region, but rather at a slightly smaller and δn_M -dependent modulation frequency $\Omega_{\text{Res}} = (1 - \delta n_M^2/8)\omega_p/n$. Moreover, notwithstanding the n -dependence of the location resonances of this type, (10) is *completely independent of n* , in contrast with (9), with a *common* maximal growth exponent $\omega''_{\text{Res}} = \omega_p\delta n_M^2/4$, which is quadratic in δn_M , and is therefore of higher order in perturbation theory.

B. The Effect of Dissipation - Numerical Results

The discussion in the main text focused on lossless systems, $\nu = 0$. For completeness, in Fig.S2 we demonstrate schematically the effect of turning the damping coefficient ν on.

This figure shows the locus of the eigenfrequencies $\omega' + i\omega''$ in the complex plane, for values of the loss parameter ν in the range $0 < \nu < 5\omega_p$. The direction of increasing loss is indicated by arrows. The modulation frequency is $\Omega = 2\omega_p$ and $\delta n_M = 0.5$. At $\nu = 0$, one of the eigenfrequencies resides in the upper half of the frequency plane, represented by the upper endpoints of the curves (note that due to the periodicity of the band diagram in ω' the two endpoints represent the same eigenfrequency). Its counterpart (not shown in the figure), is located symmetrically across the $\omega'' = 0$ horizontal axis. As the dissipation parameter increases, both modes descend towards the lower-half frequency plane, eventually converging in a bifurcation. The eigenfrequency of the mode experiencing gain intersects the $\omega'' = 0$ line when ν is approximately $0.32\omega_p$, highlighting a critical transition point influenced by dissipation. For comparison, the green points represent a similar study for the case when the modulation strength is vanishingly small ($\delta n_M \approx 0$). As expected, in this case the spectrum lies completely in the lower-half frequency plane.

C. Dirac Comb of δ -Impulses

Going back to the more general piecewise constant profile (with $\tau \neq T/2$, that is, uneven durations of the two constant values of the modulation amplitude δn), an interesting limit is obtained when, for example, we let $\tau \rightarrow 0^+$, $n_1 \propto 1/\tau$ and $n_2 = 0$. In this limit we obtain a Dirac comb of δ -impulses, namely,

$$\delta n(t) = \alpha \sum_{j=1}^{\infty} \delta(t - jT) \quad (11)$$

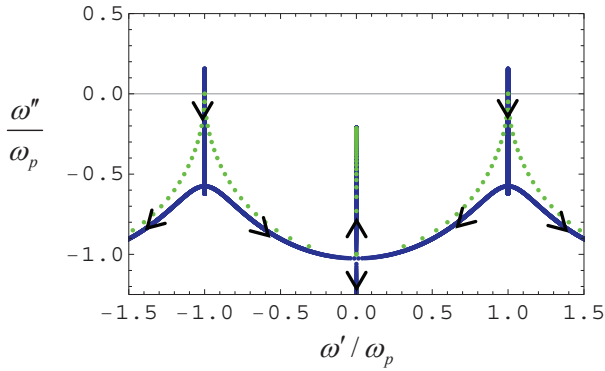


FIG. S2: Locus of $\omega' + i\omega''$ in the complex plane as a function of the damping strength ν at modulation frequency $\Omega = 2\omega_p$. The arrows indicate the direction of increasing ν . i) $\delta n_M = 0.5$ (solid blue lines), ii) $\delta n_M = 0^+$ (green dots). The horizontal grid line (in gray) separates the stable and unstable regions.

with time-independent parameters α and T . With this type of modulation, Eq. (1) is conveniently solved by computing explicitly the transfer matrix \mathbf{T} (in the ‘scattering basis’), as we now explain. Between impulses, say for $jT < t < (j+1)T$, $f(t)$ evolves as a linear combination $A_j e^{-i\omega_+(t-jT)} + B_j e^{-i\omega_-(t-jT)}$ of the two frequencies $\omega_{\pm} = -i\nu/2 \pm \omega'_p$ of the time-independent problem, with $\omega'_p = \sqrt{\omega_p^2 - \nu^2/4}$, under the further assumption that ω'_p is real-valued, namely, that the system is not overdamped. The solution $f(t)$ is continuous throughout the impulse at $t = (j+1)T$, while $\partial_t f$ suffers a jump discontinuity: $\partial_t f_+ - \partial_t f_- = -\alpha \omega_p^2 f$ (with obvious notations).

These properties uniquely determine the amplitudes A_{j+1} and B_{j+1} right after a given impulse as $(A_{j+1}, B_{j+1})^T = \mathbf{T}(A_j, B_j)^T$ where⁷

$$\mathbf{T} = e^{-\frac{\nu T}{2}} \begin{pmatrix} 1 - iu & -iu \\ iu & 1 + iu \end{pmatrix} \begin{pmatrix} e^{-i\theta} & 0 \\ 0 & e^{i\theta} \end{pmatrix} \quad (12)$$

with $u = \frac{\alpha \omega_p^2}{2\omega_p}$ and $\theta = \omega'_p T$. The eigenvalues of \mathbf{T} control stability of the system, namely, whether the amplitudes grow (regions of instability in parameter space) or remain bounded (regions of stability). For simplicity, let us analyze the stability properties of the PLTC in the absence of damping ($\nu = 0$), where $u = \frac{\alpha \omega_p}{2}$.

In this case $\det \mathbf{T} = 1$ and the two mutually reciprocal eigenvalues of \mathbf{T} are $\Lambda_{\pm} = \text{Tr} \mathbf{T}/2 \pm \sqrt{(\text{Tr} \mathbf{T}/2)^2 - 1}$, where $\text{Tr} \mathbf{T}/2 = \text{Re} T_{11} = \cos \theta - u \sin \theta$.

Thus, if $|\text{Re} T_{11}| > 1$, both eigenvalues are real, with either $|\Lambda_+|$ or $|\Lambda_-| > 1$, resulting in the growth of $f(t)$ after each kick. This is the region of instability. If, on the other hand, $|\text{Re} T_{11}| < 1$, then $\Lambda_- = \Lambda_+^*$ so that $|\Lambda_{\pm}| = 1$ and $f(t)$ remains bounded as function of time. This is the region of stability. Clearly, the boundaries separating regions of stability and instability are determined by $\cos \theta - u \sin \theta = \pm 1$. Such points

in the parameter space of \mathbf{T} are exceptional points, where the matrix is non-diagonalizable, possessing only a single eigenvector. Straightforward calculation shows that

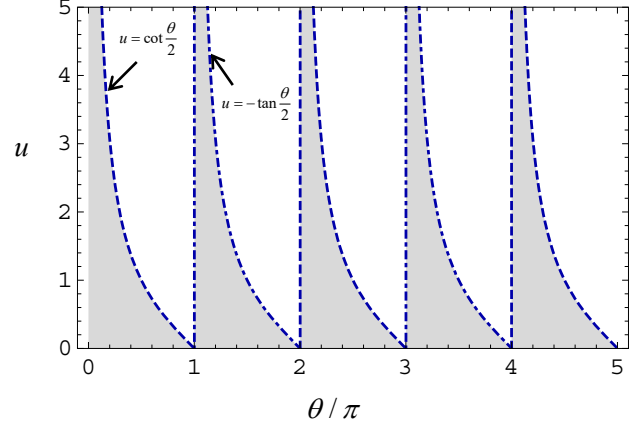


FIG. S3: Stability region of the $u - \theta$ plane for the Dirac impulse model (11). The zone shaded in gray is the stability region in parameter space. The boundary curves are determined by $u = \cot \theta/2$ (dashed curves) and $u = -\tan \theta/2$ (dot dashed curves).

at the instability threshold u and θ are related either by $u = \cot \theta/2$ (when $\text{Tr} \mathbf{T}/2 = -1$) or $u = -\tan \theta/2$ (when $\text{Tr} \mathbf{T}/2 = 1$). Let us denote the border stability lines of the first type by $\theta_-(u)$, and the border stability lines of the second type by $\theta_+(u)$. As illustrated in Fig.S3, the stability regions are the areas lying between these curves and the horizontal axis in the $u - \theta$ plane. The curves $\theta_-(u)$ terminate on the horizontal axis of Fig.S3 at points where $\theta/\pi = \text{an odd integer}$, whereas the curves $\theta_+(u)$ terminate there at points where $\theta/\pi = \text{an even integer}$. Let us consider now narrow strips in the unstable region immediately to the right of the border lines. That is, for a given u , we set $\theta = \theta_{\pm}(u) + \Delta$ with $0 < u\Delta \ll 1$. By expressing $\sin \theta_{\pm}(u)$ and $\cos \theta_{\pm}(u)$ in terms of u , it is straightforward to show in these strips that $\cos(\omega T) = \text{Tr} \mathbf{T}/2 = \pm(\cos \Delta + u \sin \Delta) \simeq \pm \cosh(\sqrt{2u}\Delta)$. Thus, immediately on the right of both lines $\theta_{\pm}(u)$ the instability growth rate is $\omega'' = \sqrt{2u}\Delta/T$, but such generic instability is non-resonant (in the sense that it does not have a local maximum as function of Δ). Resonances naturally appear near the horizontal axis in Fig.S3, where the ‘tongues’ of instability terminate, that is where also $\theta/\pi = n$ an integer. (We remind the reader that odd integers correspond to the $\theta_-(u)$ lines, and even integers to the $\theta_+(u)$ lines.) Thus, for $u \sim \Delta \ll 1$ we obtain $\cos(\omega T) = \pm(\cos \Delta + u \sin \Delta) \simeq (-1)^n \cosh(\sqrt{u^2 - (\Delta - u)^2}) + \mathcal{O}(\Delta^4, u\Delta^3)$. Therefore, in the vicinity of a given $\theta \simeq n\pi$ in the $u - \theta$ plane, the resonance is centered at $\Delta = u$ (that is, at $\theta_{\text{Res}} = \theta_{\pm}(u) + u$), with maximal growth rate

$$\omega''_n = \frac{u}{T} = \frac{\Omega u}{2\pi}, \quad (13)$$

independently of n . The real part of the Floquet frequency depends on the parity of n . Thus, $\omega' = 0$ for resonances corresponding to even n , while $\omega' = \pm\pi/T = \pm\Omega/2$ (in the first Brillouin zone) for resonances corresponding to odd n .

Finally, as can be seen in Fig.S3, the system is always unstable in the vicinity of $\theta_n = n\pi + 0^-$ (with integer n), which corresponds to modulation frequency $\Omega_n = 2\omega_p/n$. Furthermore, as $u \rightarrow 0+$ (no impulses) the gaps disappear, rendering the system always stable, while in the opposite limit $u \rightarrow +\infty$ the stability regions shrink to the points $\theta_n = n\pi + 0^+$.

IV. PARAMETRIC RESONANCES AT WEAK MODULATION - THE GENERAL CASE

We shall now offer a very simple demonstration of the existence of parametric resonances for generic periodic modulation at frequencies $\Omega = 2\omega_p/n$ with integer n , and derive the corresponding growth exponents at these resonances (i.e., at zero detuning Δ) given by Eq.(13) in the main text. For simplicity, we limit the discussion to the non-dissipative case $\nu = 0$. To this end, we consider the system of equations (3), where now $\psi_1 = \omega_p f(t)$ and $\psi_2 = \dot{f}(t)$. We further assume that the weak modulation $\delta n(t)$ oscillates equally between positive and negative values, so that its zeroth Fourier component $c_0 = \int_0^T \delta n(t) dt / T = 0$ (i.e., its mean value) vanishes.

In the absence of modulation ($\delta n = 0$), Eq.(3) is identical in form to the Schrödinger equation for a spin-1/2 (with magnetic moment normalized to 2) precessing in a constant magnetic field $\mathbf{B} = -\omega_p \hat{y}$, whose eigen-solutions are

$$\Psi_{\pm}(t) = \frac{1}{\sqrt{2}} \begin{pmatrix} 1 \\ \pm i \end{pmatrix} e^{\pm i\omega_p t} \quad (14)$$

and with corresponding eigenvalues $\mp\omega_p$. Now we turn the modulation on, and in the spirit of the discussion in⁸ of parametric resonances in the Mathieu equation, seek a solution of (3) in the form $\Psi(t) = (\psi_1, \psi_2)^T = a(t)\Psi_+(t) + b(t)\Psi_-(t)$, with *slowly varying* amplitudes $a(t)$ and $b(t)$, which serve as amplitude envelopes to the harmonically oscillating factors. (This is reminiscent of transforming to the interaction picture in Quantum Mechanics.) Thus, if $f(t) = \psi_1(t)/\omega_p$ is the Floquet eigen-solution of the equation with eigenvalue $\Lambda = e^{-i(\omega' + i\omega'')T}$, then the growth (or decay) coefficient ω'' should be encoded in the exponential envelope of $a(t)$ and $b(t)$, while the oscillatory parts of the latter should combine with the phase factors $e^{\pm i\omega_p t}$ in (14) to produce the real part ω' of the Floquet frequency. By substituting this form of $\Psi(t)$ in (3) and utilizing orthonormality of the eigenspinors

(14) we obtain the equation for $a(t)$ and $b(t)$ as

$$\frac{d}{dt} \begin{pmatrix} a(t) \\ b(t) \end{pmatrix} = i \frac{\omega_p \delta n(t)}{2} \begin{pmatrix} 1 & e^{-2i\omega_p t} \\ -e^{2i\omega_p t} & -1 \end{pmatrix} \begin{pmatrix} a(t) \\ b(t) \end{pmatrix}. \quad (15)$$

This equation is exact. In what follows we shall assume the modulation $\delta n(t)$ is very weak, and contend ourselves with solving (15) perturbatively to leading order in $\delta n(t)$.

By assumption, $\delta n(t)$ oscillates evenly between positive and negative values, and its oscillations are in general incommensurate with those of the phases $e^{\pm 2i\omega_p t}$. In our perturbative solution of (15), we have to integrate its right-hand over a period of time t (starting at some initial time t_0). Let us assume t contains many modulation cycles. For generic modulation $\delta n(t)$ it is plausible to expect significant cancellations (or ‘destructive interference’) in this integral. Therefore, this integral should be dominated by the least oscillating terms in the quantities ($\delta n(t) \exp \pm 2i\omega_p t$) in the integrand, which must be a combination of an appropriate Fourier mode of $\delta n(t)$ and the phases $e^{\pm 2i\omega_p t}$. Thus, we substitute the Fourier decomposition $\delta n(t) = \sum_{l=1}^{\infty} (c_l \exp(i l \Omega t) + c_l^* \exp(-i l \Omega t))$ in (15) and average it over one modulation period. In this procedure we encounter integrals of the form $(1/T) \int_0^T dt \exp[\pm i(l\Omega - 2\omega_p)t]$, whose phase is minimized for the pair of Fourier modes corresponding to $l = [2\omega_p/\Omega]$ (where $[x]$ is the integral part of the real number x). In particular, if Ω and $2\omega_p$ are commensurate such that $\Omega = 2\omega_p/n$ with integer n , this minimal phase, occurring for $l = n$ will be exactly null, and the dominant part in (15) will be

$$\frac{d}{dt} \begin{pmatrix} a(t) \\ b(t) \end{pmatrix} = \frac{\omega_p}{2} \begin{pmatrix} 0 & ic_n \\ -ic_n^* & 0 \end{pmatrix} \begin{pmatrix} a(t) \\ b(t) \end{pmatrix}, \quad (16)$$

with eigenvalues $\pm\omega_p |c_n|/2$, leading to growth exponent

$$\omega'' = \frac{\omega_p |c_n|}{2} \quad (17)$$

for the instability at modulation frequency $\Omega = 2\omega_p/n$. This result is linear in c_n , and therefore in δn by construction. Thus, any such parametric resonance is one of the set of *dominant* resonances for the modulation profile $\delta n(t)$, analogous to the one associated with (9) in the case of piecewise constant modulation.

We comment that in the averaging procedure leading to (16) we have obviously lost all information about the oscillatory behavior of the amplitudes $a(t)$ and $b(t)$, and in particular, of the real part ω' of the Floquet frequency corresponding to this resonance. Indeed, the (approximate) amplitudes $a(t)$ and $b(t)$ resulting from (16) are not oscillatory and have purely real exponential behavior $e^{\pm\omega'' t}$. The only oscillatory part of the full solution for $\Psi(t) = (\psi_1(t), \psi_2(t))^T$ comes from the phases $e^{\pm i\omega_p t}$ in (14), which are independent of $\delta n(t)$

and therefore of the modulation frequency Ω . Indeed, the approximate growing (unstable) solution arising from (16) and (17) is $(a(t), b(t))^T \simeq (1, -i)^T e^{\omega'' t}$, leading to $(\psi_1, \psi_2)^T = (\omega_p f(t), \dot{f}(t)) \simeq (\cos \omega_p t, -\sin \omega_p t) e^{\omega'' t}$ (where a term of order $\omega''/\omega_p \propto |c_n|$ was neglected in the component $\psi_2 = \dot{f}$). Thus, the cosine factor in $f(t)$ oscillates periodically at frequency $\omega_p = n\Omega/2 \neq \Omega$, and is therefore not even a proper Floquet solution (unless $n = 2$ accidentally). Therefore, the averaged ‘hamiltonian’ (16) should only be used to determine the exponential envelope of the Floquet eigensolutions.

For example, in the Mathieu case (Eq.(8) in the main text), $c_l = (\delta n_M/2)\delta_{l,1}$, so there is only one dominant resonance which occurs for $n = 1$ at $\Omega = 2\omega_p$ and with the known growth exponent $\omega'' = \omega_p \delta n_M/4$.

For the piecewise constant modulation (5), the Fourier modes are $c_n = 0$ for even n and $c_n = 2\delta n_M/\pi i n$ for odd values of n . Thus, there is an *infinite set of dominant resonances* at modulation frequencies $\Omega = 2\omega_p/n$ with n an odd number, with corresponding growth exponents $\omega'' = \omega_p \delta n_M/\pi n$, which agrees with the result (9) obtained directly from the dispersion relation (7). There are no *dominant* resonances corresponding to n even simply because there are no Fourier modes of even order for the modulation (5), as we discovered by direct analysis of (8).

Finally, for the Dirac-comb impulse modulation (11), the Fourier modes are $c_n = \frac{\alpha}{T} = \frac{2u}{\omega_p T}$, independently of n , and indeed, we see from (13) and (17) that $\omega'' = \frac{u}{T} = \frac{\omega_p |c_n|}{2}$.

In order to determine higher order resonances of the modulated system, that is, resonances with growth exponents ω'' which depend on higher powers of the small amplitude δn , as those mentioned in⁸ for the Mathieu equation, or those corresponding to (10) for the piecewise constant case, one should analyze higher orders in the time-dependent perturbative expansion of the solution of (15).

V. NUMERICAL RESULTS FOR RESONANCE GROWTH RATES FOR TRANSVERSE MODULATED PLASMONS

As was discussed in the main text, the discussion of instabilities in longitudinal PLTCs can be transferred, *mutatis mutandis*, to transverse PLTCs.

In particular, the most significant instability is linked

to the interband transition at modulation frequency $\Omega_T(k) = 2\omega_T(k) = 2\sqrt{\omega_p^2 + c^2 k^2/\varepsilon_0}$, as indicated in Fig.1a in the main text. As in the case of longitudinal plasmons, we interpret this instability as arising from the interaction between negative and positive frequency branches $\pm\omega_T(k)$. However, for transverse plasmons, it is k -dependent, in contrast with the longitudinal case. Consequently, in the PLTC, the parametric gain is predominantly governed by longitudinal plasmons, which, as previously discussed, experience a collective, k independent leading resonance at $\Omega = 2\omega_p$. It is this collective resonance that determines the optimal path for gain extraction from the external driving. For completeness, we show in Fig.S4 the gain rate of transverse plasmons as a function of the modulation frequency in the case of piecewise modulation, for a particular value of k . The system parameters are as in Fig.2 in the main text, namely, strong modulation amplitude $\delta n_M = 0.5$. Note that at such strong modulation amplitudes, the locations of longitudinal resonances shift from their corresponding weak amplitude locations around $\Omega = 2\omega_p/m$ with integer m . However, as is evident from Fig.2, these shifts are bounded, and at least for the first few (longitudinal and transverse) resonances we discuss specifically in this section, there is no risk of confusion among resonances by referring to the corresponding locations at weak amplitude modulation. Having said that, we see in Fig.S4 that the gain rate for $k = 0$ coincides with the gain rate of the longitudinal plasmons (solid blue curves). (Shown in Fig.S4 are the two resonances corresponding to values $m = 1, 2$ of Fig.2 at $\Omega = 2\omega_p$ and ω_p , respectively.) For nonzero k the gain peaks are blue-shifted (dashed black curves) to $\Omega = 2\omega_T/m > 2\omega_p/m$ with integer m . According to the discussion around Eq.(15) in the main text, we can relate the resulting resonances to those arising in a longitudinal PLTC with effectively smaller amplitude $\omega_p^2 \delta n_M/\omega_T^2$, which would generate a smaller growth rate compared to the longitudinal case as k increases. For the particular chosen value of k in Fig.S4 we have $\omega_T = \sqrt{2}\omega_p$. As expected, the displayed dashed curves, indicating transversal resonances are centered near the dashed vertical lines at $\Omega/\omega_p = 2\sqrt{2}, \sqrt{2}$ and $2\sqrt{2}/3$, corresponding to the predicted (weak amplitude locations) at $2\omega_T/m$ with $m = 1, 2, 3$. As is also evident from Fig.S4, the peak gain for the transversal resonances at $k \neq 0$ are smaller compared to their counterparts in Fig.2, which is consistent with the effective reduction of the effective modulation amplitude, as discussed above.

¹ L. Brillouin, *Wave Propagation in Periodic Structures - Electric Filters and Crystal Lattices*, (McGraw Hill Book Company, New York, 1946), Chapter 8.

² B. van der Pol and M. J. O. Strutt, *On the Stability of the Solutions of Mathieu's Equation*, Phil. Mag. **5** 18 (1928).

³ W. Magnus and S. Winkler, *Hill's Equation*, (Dover Publications, New York, 2004).

⁴ J. C. Serra, M. G. Silveirinha, *Homogenization of Dispersive Spacetime Crystals: Anomalous Dispersion and Negative Stored Energy*, Phys. Rev. B **108**, 035119, (2023).

⁵ F. R. Prudêncio and M. G. Silveirinha, *Synthetic Axion Response with Spacetime Crystals*, Phys. Rev. Appl. **19**,

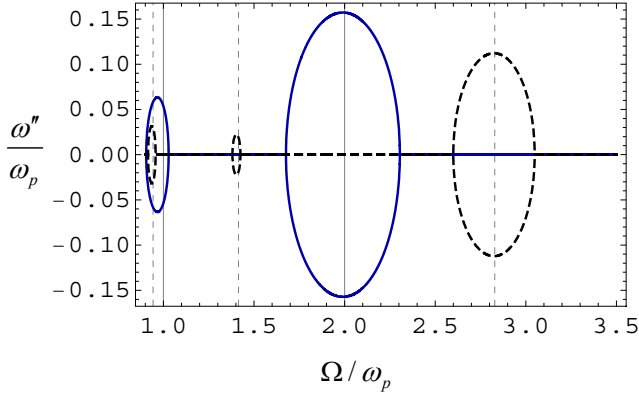


FIG. S4: Amplification rate as a function of the modulation frequency for the same system as in Fig.2 in the main text. Solid blue lines: longitudinal plasmons and transverse plasmons with $k = 0$. Dashed black lines: Transverse plasmons with $k = \sqrt{\varepsilon_0}\omega_p/c$, that is, $\omega_T(k) = \sqrt{2}\omega_p$. The two solid vertical gridlines coincide with their counterparts at $\Omega/\omega_p = 1, 2$ in Fig.2 in the main text. The dashed vertical lines indicate modulation frequencies $\Omega = 2\omega_T/m = 2\sqrt{2}\omega_p/m$ for $m = 1, 2, 3$.

024031, (2023).

⁶ I. Kiropelidis, F. K. Diakonou, G. Theocharis, and V. Pagneux, *Transient amplification in Floquet media: the Mathieu oscillator example*, arXiv:2404.00138 (2024).

⁷ R. Carminati, H. Chen, R. Pierrat, and B. Shapiro, *Universal Statistics of Waves in a Random Time-Varying Medium*, Phys. Rev. Lett. **127**, 094101 (2021).

⁸ L. D. Landau and E. M. Lifshitz, *Mechanics*, 3rd edition, (Pergamon Press, Oxford, 1976), section 27.